Flexoelectricity in nematic domain walls

Steve J. Elston
Department of Engineering Science, University of Oxford, Parks Road, Oxford, OX1 3JP, United Kingdom
(Received 21 September 2007; published 1 July 2008)

Flexoelectric effects are studied in the domain walls of a nematic liquid crystal device showing the Freedericksz transition. Walls parallel to the alignment direction have a strong twist distortion and an electro-optic effect dominated by e_1-e_3 is seen. Walls perpendicular to the alignment direction have a strong splay-bend distortion and an electro-optic effect dominated by e_1+e_3 is seen. This allows the study of both flexoelectric coefficient combinations in a single device.

DOI: 10.1103/PhysRevE.78.011701 PACS number(s): 61.30.−v

I. INTRODUCTION

Flexoelectricity in nematic liquid crystals was first discussed by Meyer nearly 40 years ago [1]. Since then there has been a considerable amount of work undertaken to understand, measure, and exploit the flexoelectric effect [2]. There has been renewed interest in recent years because of the potential for the exploitation of flexoelectricity in the switching of bistable display technology [3,4] and the high-speed behavior of the chiral-flexo-electro-optic effect [5].

The flexoelectric effect is a direct coupling between the molecular field of a liquid crystal and induced dipoles. The result is a distortion dependent electric polarization which can be expressed in terms of splay and bend vectors as

$$\mathbf{P}_{\text{flexo}} = e_1\mathbf{n}(\boldsymbol{\nabla}\cdot\mathbf{n}) + e_3(\boldsymbol{\nabla}\times\mathbf{n})\times\mathbf{n}, \tag{1}$$

where $\mathbf{n}$ is the nematic director, e_1 is the splay flexoelectric coefficient, e_3 is the bend flexoelectric coefficient, and $\mathbf{P}_{\text{flexo}}$ is the resulting polarization.[1] There is no twist term in the polarization because of the inversion symmetry of helical structures.

As a result of the interaction between the flexoelectric polarization and externally applied electric fields there are some interesting phenomena which are not due to the conventional coupling with the dielectric anisotropy of the liquid crystal. In his original work Meyer suggested the possibility of a periodic domain pattern containing alternate regions of bend and splay distortion [1]. In fact there are a wide range of (hydrodynamic) flexoelectric patterns possible [6], and the relation between flexoelectric domains and transient switching behavior has proven interesting [7].

There is in fact a direct link between a pattern originally suggested by Meyer and the chiral-flexo-electro-optic effect presented by Patel and Meyer [5]. In this effect an electric field is applied perpendicular to the helical axis of a chiral nematic material leading to a field dependent tilt in the optic axis in a plane containing the helix axis but orthogonal to the field direction. The chiral-flexo-electro-optic effect has received attention due to its fast, linear and in-plane electro-optic properties [8,9]. The behavior can be understood by considering a plane cutting in a direction containing the nematic molecular axis and the applied field. Under electric field application this plane effectively rotates, leading to a splay-bend distortion and a consequent flexoelectric polarization [5]. Analysis of the behavior, with the assumption that the reorientation can be represented by a single angle ϕ around an axis parallel to the applied field, leads to

$$\tan\phi = \frac{e_1-e_3}{2K_{22}Q}E - \frac{K_{11}-2K_{22}+K_{33}}{2K_{22}}\sin\phi$$

$$\Rightarrow \phi \approx \frac{e_1-e_3}{(K_{11}+K_{33})Q}E, \tag{2}$$

where Q is the magnitude of the helical pitch wave vector, E is the applied electric field (assumed uniform), and K_{11}, K_{22}, and K_{33} are the usual splay, twist, and bend elastic constants. It is notable that the effect depends on the combination of flexoelectric coefficients e_1-e_3 (often those working on this effect use the alternative convention for the flexoelectric polarization, resulting in the combination of coefficients e_s+e_b in the equation for ϕ [5]).

Flexoelectric behavior in a hybrid aligned nematic (HAN) structure (which involves planar splay-bend distortion) depends on the combination of coefficients e_1+e_3. The switching in this case can be used as an analogy to that in bistable devices [10]. HAN structures have also been used to determine values of the sum of the flexoelectric coefficients using a number of techniques [11,12]. For these structures the torque on a director tilted by an angle θ is given by

$$\text{torque} = -(e_1+e_3)\sin\theta\cos\theta\frac{\partial E}{\partial z}, \tag{3}$$

where z is the direction across the thickness of the device and θ is measured away from the aligning surfaces. It is notable that this torque term involves field gradients [13].

In general, for an electric field $\mathbf{E}$ the bulk torque can be written in terms of the molecular field, giving a flexoelectric torque $\Gamma_f^b=\mathbf{n}\times\mathbf{h}_f$, where $\mathbf{h}_f$ is of the form [2]

$$\mathbf{h}_f = (e_1-e_3)[\mathbf{E}(\boldsymbol{\nabla}\cdot\mathbf{n}) - (\boldsymbol{\nabla}\otimes\mathbf{n})\mathbf{E}] - (e_1+e_3)(\mathbf{n}\cdot\boldsymbol{\nabla})\mathbf{E}. \tag{4}$$

From this it can be seen that bulk flexoelectric torques appear in two terms: (i) a term in e_1-e_3 which is related to gradients in the director, and is the only term when the field is uniform (as assumed in the chiral-flexo-electro-optic case);

[1] Note that in some work the flexoelectric polarization is written as $\mathbf{P}_{\text{flexo}}=e_s\mathbf{n}(\boldsymbol{\nabla}\cdot\mathbf{n})+e_b\mathbf{n}\times(\boldsymbol{\nabla}\times\mathbf{n})$ which is equivalent to Eq. (1) under the conditions $e_s=e_1$ and $e_b=-e_3$.

(ii) a term in e_1+e_3 which is related to gradients in fields (it is generally the only bulk term when the director and field are coplanar, as in the HAN case). Although sum and difference terms are seen to be important in the cases discussed above it is additionally interesting to consider further structures in which such terms can be observed.

II. DOMAIN WALLS

In the well know Freedericksz transition in nematic liquid crystals [14] there is a degeneracy in the induced tilt direction under field application. In general this is observed for so-called parallel aligned liquid crystal devices but not for antiparallel aligned. In the latter case the net pretilt in the director orientation (before field application) ensures that when a field is applied all director reorientation takes place homogeneously. However, in parallel aligned cells the initial net pretilt is zero and the result is that under field application two different director reorientation processes take place. Experimentally this can be observed as domain formation, as seen in the polarizing microscope image shown in Fig. 1(a). Here the regions inside the domains and outside the domains have reoriented in opposite senses, with the domain wall being the interface between regions. This can be best understood by illustrating the director structures involved.

Figure 2 shows a model of the structure in the vicinity of a domain wall, where the cross section shown is taken parallel to the alignment direction and the wall is running perpendicular to this direction. The region to the left is "seeded" to switch in one reorientation direction and the region to the right is "seeded" to switch in the opposite sense (this is done by slightly breaking the symmetry of the surface conditions in these two regions). Here the director remains in the plane of the illustration and the domain wall has a splay-bend structure. Although the wall enclosing a domain of reorientation is always the interface between the tilted reorientation states seen in Fig. 2 the detailed structure of the wall varies from place to place. For example, at a point where the domain wall runs parallel to the alignment direction the structure of the interface region is somewhat different from that discussed above. This can be seen by comparing Fig. 2 with the structure model shown in Fig. 3(a), which is obtained by taking a cross section perpendicular to the alignment direction in the vicinity of a wall running parallel to it. In this case the director tilt in the two domains is out of the plane of the illustration, making the structure slightly harder to visualize. However, the structure becomes clear if a cross section line is taken through the midplane of the structure viewed from above. This is shown in Fig. 3(b), which indicates that in this case the wall is basically a twist structure.

In fact, because the twist elastic constant for a nematic material (K_{22}) is generally smaller than the splay and bend constants (K_{11} and K_{33}) twist structures are of lower energy. This causes the domains to be oval (otherwise round domains might be expected) and also means that the splay-bend distortion is limited to a small region where the wall is perpendicular to the alignment direction. Such behavior can be seen in Fig. 1(b) which shows part of the domain wall when the device is oriented so that the bulk alignment shows extinction. There is only a small region where the wall is dark, indicating in-plane splay-bend distortion.

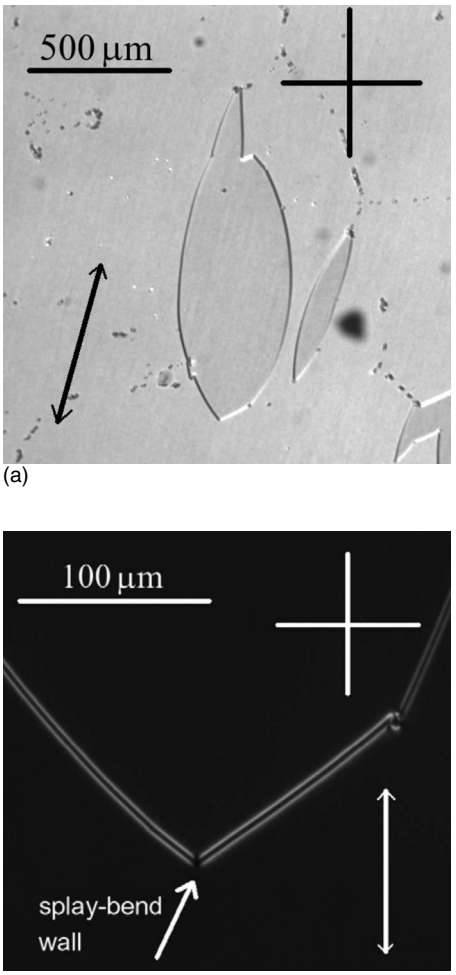

FIG. 1. (a) Polarizing microscope image of domain formation during the Freedericksz transition in a parallel aligned nematic liquid crystal device with a voltage of 2 V ac between the cell electrodes. When a field is applied the direction of tilt reorientation is degenerate, and the regions inside and outside of the domains have switched in opposite senses. The domains are stabilized because the walls get pinned by spacer balls within the device. (The surface alignment orientation is indicated by the double ended arrow and the polarizer/analyzer orientations by the + symbol.) (b) Polarizing microscope image of a domain wall when the device is oriented to show extinction between crossed polarizers. The point at which the wall has a splay-bend structure also shows extinction and is indicated by the arrow on the image. (The surface alignment orientation is indicated by the double ended arrow and the polarizer and analyzer orientations by the + symbol.)

It is interesting to consider the structure of the domain walls together with the earlier comments made on flexoelectricity. The director in splay-bend walls remains in one plane, and in addition there will be field gradients in this plane due to the dielectric anisotropy of the non-uniform structure. These are the conditions outlined above for a flexoelectric torque dependent on the sum of the coefficients e_1+e_3. However, the structure in the twist wall is similar to a small

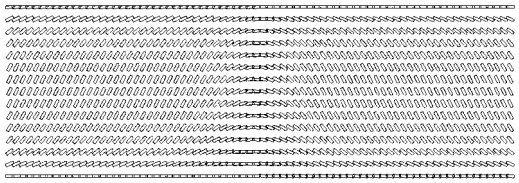

FIG. 2. A model of the director structure in a splay-bend domain wall. The region to the left has been seeded to switch in one reorientation direction and the region to the right in the opposite direction. The interface region is the domain wall structure at the point indicated in Fig. 1(b) and the cross section is taken parallel to the alignment direction (perpendicular to the wall direction at this point).

segment of helix in a chiral-flexo-electro-optic arrangement. Therefore, in this case, we might expect a flexoelectrically induced reorientation dependent on the difference of the coefficients $e_1 - e_3$ [i.e., behavior similar to that defined in Eq. (2) above]. In the discussion below modeling of this behavior is presented, together with experimental observations.

III. MODEL

By dealing only with cross sections perpendicular to a domain wall the problem under consideration becomes two dimensional. A coordinate system is chosen with z being the direction across the thickness of the liquid crystal layer and x being the direction in the plane of the device surfaces, orthogonal to the local domain wall. The director is $\mathbf{n} = (n_x, n_y, n_z)$, and the position-dependent potential is V. All variables are functions of x and z only, being independent of the y direction (the direction parallel to the local domain wall). The bulk energy density is then

$$f = \frac{1}{2}\{K_{11}(\boldsymbol{\nabla}\cdot\mathbf{n})^2 + K_{22}(\mathbf{n}\cdot\boldsymbol{\nabla}\times\mathbf{n})^2 + K_{33}(\mathbf{n}\times\boldsymbol{\nabla}\times\mathbf{n})^2\}$$

$$-\frac{1}{2}\Delta\epsilon\epsilon_0(\mathbf{n}\cdot\mathbf{E})^2 - \mathbf{P}_{\text{flexo}}\cdot\mathbf{E}, \tag{5}$$

where $\Delta\epsilon$ is the dielectric anisotropy and other terms have been defined above. In the two-dimensional system under consideration expansion of the flexoelectric polarization [Eq. (1)] gives

$$\mathbf{P}_{\text{flexo}} = e_1\left(\frac{\partial n_x}{\partial x} + \frac{\partial n_z}{\partial z}\right)\begin{pmatrix} n_x \\ n_y \\ n_z \end{pmatrix} + e_3\begin{pmatrix} n_z\left(\frac{\partial n_x}{\partial z} - \frac{\partial n_z}{\partial x}\right) - n_y\frac{\partial n_y}{\partial x} \\ n_x\frac{\partial n_y}{\partial x} + n_z\frac{\partial n_y}{\partial z} \\ -n_y\frac{\partial n_y}{\partial z} - n_x\left(\frac{\partial n_x}{\partial z} - \frac{\partial n_z}{\partial x}\right) \end{pmatrix}. \tag{6}$$

Some care needs to be taken in the determination of the local electric field because it can be influenced by both dielectric anisotropy and flexoelectric polarization. However, the field can be obtained by first finding a solution to Poisson's equation in the form

$$\boldsymbol{\nabla}\cdot(-\epsilon_0\underline{\underline{\epsilon}}\,\boldsymbol{\nabla}V + \mathbf{P}_{\text{flexo}}) = 0, \quad \underline{\underline{\epsilon}} = \epsilon_{ij} = \epsilon_\perp\delta_{ij} + \Delta\epsilon n_i n_j, \tag{7}$$

where $\epsilon_\perp$ is the relative permittivity perpendicular to the director, and the electrode voltages set the boundary conditions on V. (The director components are represented by $n_1 = n_x$, $n_2 = n_y$, and $n_3 = n_z$) Knowledge of V then allows the field to be found from $\mathbf{E} = -\nabla V$, which can be seen from Eq. (7) to be nonuniform if the dielectric tensor $\underline{\underline{\epsilon}}$ and/or the flexoelectric polarization $\mathbf{P}_{\text{flexo}}$ are themselves nonuniform, which will be the case for the structures illustrated above.

The terms in Eqs. (5) and (7) for the system under consideration here are explicitly written out in the Appendix. In order to calculate the director structure a set of Euler-Lagrange equations for n_x, n_y, and n_z are determined from the energy density [i.e., from Eq. (5)]. (Although not complex in principle, these equations have many terms and are therefore not reproduced here. They can, however, be easily reproduced from the equations in the Appendix.) These Euler-Lagrange equations are then solved on a regular grid using a simple relaxation method. In order to work out the potential distribution (and hence $\mathbf{E}$) from Poisson's equation the same method is also used. Using a simple relaxation approach is suitable here because both the director structure and potential are smooth and continuous.

Initially the case when the externally applied electric field is ac of a frequency where dielectric interactions dominate over flexoelectric effects is considered (i.e., a frequency in the kHz range). In this situation the flexoelectric coupling in the energy density (5) can be ignored and therefore it is not necessary to include the flexoelectric terms in the Euler-Lagrange equations. Taking this approach allows the structures of the domains walls seen in Fig. 1 to be modeled, and it is these which are illustrated in Figs. 2 and 3. For the splay-bend wall structure (Fig. 2) the director at the surface is constrained to be in the x-z plane. In the region to the left of the wall in Fig. 2 the director at the lower surface is in the x direction and the director at the upper surface is tilted from

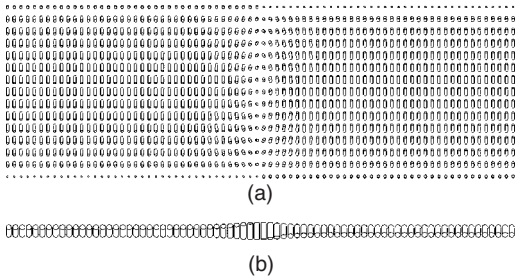

FIG. 3. (a) A model of the director structure in the vicinity of a domain wall running parallel to the alignment direction. The regions to the left and right have switched in opposite reorientation directions and the interface now has a twist structure. (b) A cross section through the center of the director structure shown in (a), viewed from above. This clearly shows the twist structure, which is similar to a small segment of a chiral nematic. Behavior analogous to that seen in the chiral-flexo-electro-optic effect [5] may therefore be expected.

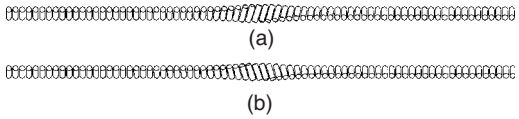

FIG. 4. (a) The change in the structure shown in Fig. 3(b) when a dc field is applied across the device leading to flexoelectrically induced distortion. Reorientation of the director within the twisted region of the wall takes place in the plane of the liquid crystal device. As expected this behavior is closely related to that seen in chiral nematics [5]. (b) The behavior of the structure when a field of opposite sign is applied.

the surface by a few degrees. In the region to the right of the wall in Fig. 2 the director at the upper surface is in the x direction and the director at the lower surface is tilted by negative a few degrees. On field application (for amplitudes greater than needed to induce the Freedericksz transition) the two regions undergo switching in opposite directions. The result of this is the formation of the splay-bend wall at the interface. For the twist wall case (Fig. 3) the director at the surface is constrained to be in the y-z plane. Again, surface pretilts are used to seed Freedericks transitions in opposite directions in the left and right regions, leading to the interface structure shown. Now the model can be used to consider how these domain wall structures are influenced by flexoelectricity by reintroducing the flexoelectric coupling terms. This will represent the behavior when the applied field is dc (or low frequency ac).

Figure 4 shows the effect on a cross section through a twist wall of including flexoelectricity and applying a positive (and negative) dc signal to a device. In comparison with Fig. 3(b) we see, as anticipated, that the region of twist within the domain wall reorients in the same manner as the structure in the chiral-flexo-electro-optic effect [5]. Adjustment of the flexoelectric coefficients shows that this effect is dependent on the combination e_1-e_3. Although field gradient effects dependent on e_1+e_3 can have a small influence on the details of the wall structure, the dominant flexoelectrically induced reorientation within the twist wall is controlled by the coefficient difference. When applied fields are small the effect is linear and the magnitude of the response appears to be consistent with the behavior described by Eq. (2), although it is not identical. For example, at the center of the structure shown in Fig. 4 the in-plane reorientation angle under field application is approximately 0.33 radians. Now the effective pitch of the helix in the middle of the domain wall illustrated in Figs. 3 and 4 can be estimated to determine the magnitude of the helical pitch wave vector and together with the flexoelectric coefficients, elastic constants, etc., this can be used in Eq. (2) to estimate the expected value of in-plane tilt. In this case the predicted tilt is 0.21 radians. This is of the same order as that determined directly within the twist wall, although is somewhat smaller. The difference is accounted for by the more complex wall structure. Nevertheless, with reasonable flexoelectric coefficients the reorientation can be several degrees and it is expected that this will be seen experimentally in microscopic images of the domain wall. The experimental observation of the twist wall behavior is discussed below.

It is also interesting to consider the behavior of the splay-bend wall (shown in Fig. 2) for dc signals when flexoelectricity is included. As anticipated this structure is uninfluenced by interaction between applied fields and flexoelectricity when the coefficients are such that the combination e_1+e_3 is zero (even though e_1-e_3 may be nonzero). But the wall structure does change due to flexoelectric interactions provided the sum of the coefficients (e_1+e_3) is not zero. Therefore the behavior confirms numerically the point noted above that when the director and field are coplanar then the only flexoelectric terms of importance are those in e_1+e_3. Provided e_1+e_3 is nonzero then the structure of the wall is slightly different under positive and negative applied signals. In particular, the effective width of the wall is dilated for one sign of field and compressed for the opposite sign of field. However, unless rather exaggerated flexoelectric coefficients are used it is difficult to see the changes in wall width in illustrations of cross sections through the director structure. Nevertheless, by examining the director tilt in the mid-plane of the cell it can be seen that changes in wall width of up to 10% (between positive and negative applied fields) may be expected. Therefore it is hoped that this can be observed experimentally in microscopic studies of the splay-bend wall behavior. These investigations are discussed below.

IV. EXPERIMENTS AND RESULTS

The device used in the experimental work consists of a parallel rubbed alignment liquid crystal cell of thickness 4.35 μm, filled with a material with the following properties: $K_{11}=10.2$ pN, $K_{22}=5.8$ pN, $K_{33}=12.7$ pN, $\Delta\epsilon=8.9$, $\Delta n=0.159$. In order to examine the behavior of a wall experimentally the intensity is plotted along a particular direction for polarizing microscope images of the type shown in Fig. 1 (referred to here as taking a line scan). Initially the line scan is taken for a splay-bend wall in the small region where the domain wall runs perpendicular to the alignment direction, at the point indicated in Fig. 1(b). To investigate the influence of flexoelectricity separate images (and line scans) are taken with positive and negative applied signals. In practice a low-frequency square wave is applied and a series of images taken, in order to minimize the influence of ions on the results. This ensures that field gradients are principally due to the effects of dielectric anisotropy. Example line scans are shown in Fig. 5(a), where the solid and dashed lines are for opposite signs of applied signal and the device is oriented at 45° to the crossed polarizers.

Using the approach to director structure modeling outlined above, together with a simple extended Jones routine to model the optical properties [15] the predicted transmission intensity for the splay-bend wall behavior is shown in Fig. 5(b). This shows the same behavior as the experimental results in Fig. 5(a), with opposite signs of applied signal leading to slightly different wall widths as observed. However, there are also some differences between the theoretical and experimental results. In both the experimental and theoretical case the wall appears as two dips in transmission with a peak in the center. This basic structure is dictated by the thickness

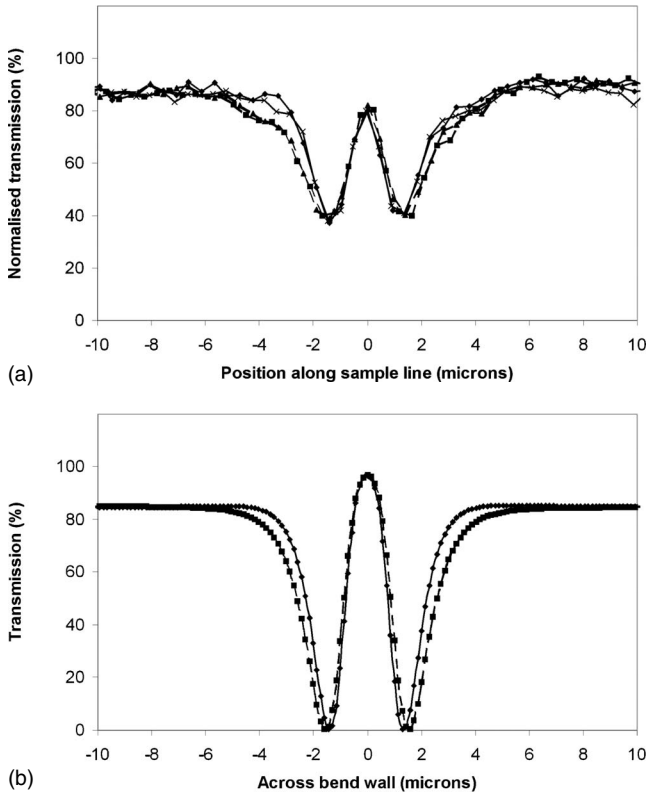

FIG. 5. (a) Transmission through the splay-bend wall extracted by plotting intensity along a line within polarizing microscope images (taking a line scan). Line scans are taken along the alignment direction, perpendicular to the local wall direction, at the point indicated in Fig. 1(b), with polarizers at ±45° from the alignment direction. The two data sets with solid lines have one sign of applied field (+2 V) and the two data sets with dashed lines have the opposite applied field (–2 V). (b) Calculated transmission line-scans for the splay-bend wall, using the methods outlined in the main text. The two lines shown have opposite signs of applied field (positive and negative 2 V in this case). In general the behavior of data shown in (a) is reproduced, with some small differences (due principally to the limitations of the optical modeling methods used).

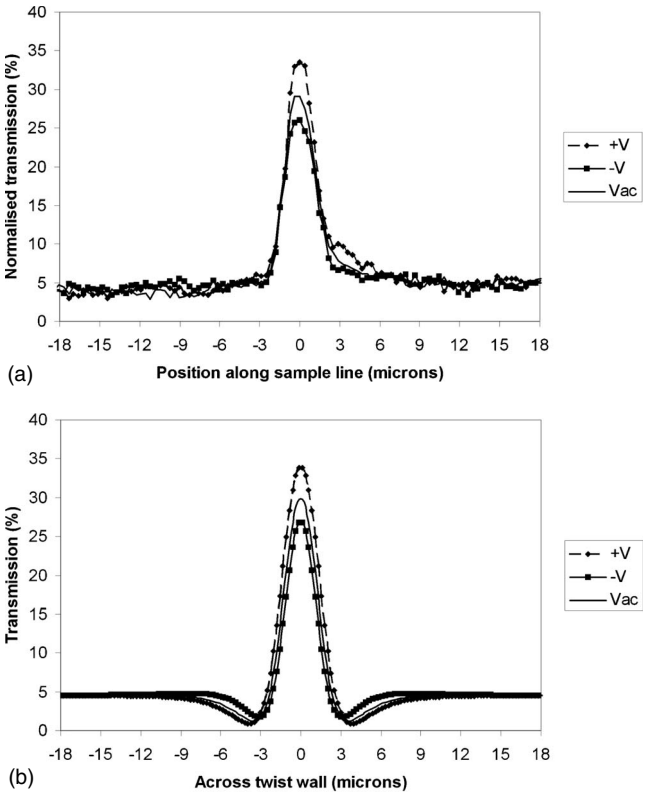

FIG. 6. (a) Transmission line scans for a twist wall, where the wall runs parallel to the alignment direction and sample lines are perpendicular to the wall. The device is oriented with the alignment direction at 22.5° to the polarizer. Data are shown with a 1.6 V r.m.s. ac signal (~ kHz), and positive and negative 1.6 V dc signals (actually extracted from low frequency square wave data). (b) Modeling line-scan data for an applied 1.6 V r.m.s. ac signal (with structure as shown in Fig. 3) and applied positive and negative 1.6 V dc signals (with structures as shown in Fig. 4). The general behavior of data shown in (a) is well reproduced.

of the device, the optical anisotropy, the voltage applied, and the dielectric anisotropy (together of course with the elastic properties of the material). From Fig. 2 we can see that in the center of the wall the structure is approximately a homogenously aligned layer, and for the device under consideration this leads to the central peak in transmission. At some point within the wall the tilt is such that the effective birefringence of the layer is equivalent to a full wave plate, whereas away from the wall the higher tilt leads to a lower birefringence (and hence higher transmission). In the theoretical modeling the position within the wall equivalent to the full wave plate condition leads to zero transmission. However, in the experiment this does not occur because (a) the light is not monochromatic, (b) there is some diffraction/scattering within the wall, and (c) the light is not collimated (due to the numerical aperture of the condenser in the polarizing microscope used). Nevertheless, although some details of the behavior are not reproduced in the model, the overall understanding appears correct and the results indicate a (magnitude) of the sum of the flexoelectric coefficients of $|e_1+e_3|=8\times10^{-12}$ C m^{-1}. This value is compatible with values others have obtained for typical materials [12].

Using a similar approach for the twist wall, but now orienting the device at 22.5° to the crossed polarizers in order to maximize the changes in transmission intensity with director reorientation in the plane of the device, results can be obtained as seen in Fig. 6(a). In this case there is little change in the wall width, but the director reorientation (seen in the modeling illustrated in Fig. 4) leads to changes in transmission for points of the image line scan within the wall. Assuming that the changes in transmission at the center of the domain wall are entirely due to the twist seen in Fig. 4 it is possible to estimate induced reorientation of the director within the plane of the device. Using transmission $\propto \sin^2(2\chi)$ where χ is the in-plane tilt angle (initially 22.5°) the total switching range between positive and negative applied fields is 3.7°. The corresponding predicted transmission behavior is shown in Fig. 6(b), which shows that the model reproduces the key effects observed, but again there are features in the data not reproduced in the model (for the reasons listed above). In this case the data and theory comparison indicates

a (magnitude) of the difference between the flexoelectric coefficients of $|e_1-e_3|=4.4\times10^{-12}$ C m^{-1}, a value not inconsistent with previous studies of standard materials [16]. We can also use this comparison to estimate the effective pitch at the center of the domain wall, which is here approximately 14 μm. However, using this together with Eq. (2) does not allow a good estimate of $|e_1-e_3|$ because of the highly nonuniform structure of the wall.

It is interesting to note that in regions of the domain wall which are neither parallel nor perpendicular to the alignment direction behavior which is dependent on a more complex combination of e_1 and e_3 may be expected (i.e., not just on the sum or difference of the coefficients). It was noted above that when the domain wall is parallel to the alignment direction there can still be some response due to e_1+e_3, but this was a rather subtle effect and the response due to e_1-e_3 dominated. However, when the domain wall is at an angle to the alignment direction then it will involve splay-bend distortion (leading to in-plane field gradients and coefficient sum behavior) and also twist structure (leading to chiral-flexo-electro-optic–type coefficient difference behavior). In these regions the effect dependent on e_1-e_3 appears to be strongest. So, in what we might term a mixed wall, the changes in transmission due to reorientation of the twist structure dominates over the rather subtle change in wall structure due to field gradient terms. In practice the field gradient term effect is quite difficult to study experimentally because it must be observed in the small region where the wall runs perpendicular to the alignment direction [seen as the region of extinction of the wall in Fig. 1(b)]. Elsewhere the field gradient effects are less significant. Therefore although it might be anticipated that e_1 and e_3 could be determined directly (rather than just the combinations e_1+e_3 or e_1-e_3) by observing and carefully analyzing the domain wall behavior in a region where it is at an oblique angle to the alignment direction in practice this is rather too difficult to achieve.

V. CONCLUSION

The effects discussed here show the influence of flexoelectric coupling on the structure of a domain wall in a nematic liquid crystal device undergoing a Freedericksz transition. The region of the wall running parallel to the alignment direction has a predominantly twist structure, and a response similar to that in the chiral-flexo-electro-optic effect is seen. This leads to in-plane rotation and depends on the flexoelectric coefficient difference (e_1-e_3). Where the wall runs perpendicular to the alignment direction the splay-bend structure leads to electric field gradients in the plane of the director. Behavior is then dependent on the coefficient sum (e_1+e_3). In principle, these results can be combined to make independent measurements of e_1 and e_3, although the measurement accuracy may not be high. It is also possible to determine the signs of these terms provided it is know which tilt states are either side of the wall being observed (i.e., which tilt state is inside and which tilt state is outside of the domain). Although not done here, this should be possible by using off-axis illumination.

In the future, work will be extended to undertake more detailed experiments, using monochromatic collimated light to ensure that images obtained can be compared directly with predications. In addition, a more careful analysis will be undertaken using finite-difference time-domain and/or beam propagation methods to model the optical properties of the domain walls.

APPENDIX

In the main text the bulk energy density is expressed by Eq. (5):

$$f=\frac{1}{2}\{K_{11}(\boldsymbol{\nabla}\cdot\mathbf{n})^2+K_{22}(\mathbf{n}\cdot\boldsymbol{\nabla}\times\mathbf{n})^2+K_{33}(\mathbf{n}\times\boldsymbol{\nabla}\times\mathbf{n})^2\}$$
$$-\frac{1}{2}\Delta\epsilon\epsilon_0(\mathbf{n}\cdot\mathbf{E})^2-\mathbf{P}_{\text{flexo}}\cdot\mathbf{E}.$$

For the two-dimensional system under consideration here the terms within this energy density equation can be expressed as

$$(\boldsymbol{\nabla}\cdot\mathbf{n})^2=\left(\frac{\partial n_x}{\partial x}+\frac{\partial n_z}{\partial z}\right)^2,$$

$$(\mathbf{n}\cdot\boldsymbol{\nabla}\times\mathbf{n})^2=\left(-n_x\frac{\partial n_y}{\partial z}+n_z\frac{\partial n_y}{\partial x}\right)^2,$$

$$(\mathbf{n}\times\boldsymbol{\nabla}\times\mathbf{n})^2=n_z^2\left(\frac{\partial n_x}{\partial z}-\frac{\partial n_z}{\partial x}\right)^2+\left(n_x\frac{\partial n_y}{\partial x}+n_z\frac{\partial n_y}{\partial z}\right)^2$$
$$+n_x^2\left(\frac{\partial n_x}{\partial z}-\frac{\partial n_z}{\partial x}\right)^2,$$

$$(\mathbf{n}\cdot\mathbf{E})^2=\left(n_x\frac{\partial V}{\partial x}\right)^2\left(n_z\frac{\partial V}{\partial z}\right)^2,$$

$$\mathbf{P}_{\text{flexo}}\cdot\mathbf{E}=-e_1\left(\frac{\partial n_x}{\partial x}+\frac{\partial n_z}{\partial z}\right)\left(n_x\frac{\partial V}{\partial x}+n_z\frac{\partial V}{\partial z}\right)$$
$$-e_3\left(\frac{\partial V}{\partial x}\left(n_z\left(\frac{\partial n_x}{\partial z}-\frac{\partial n_z}{\partial x}\right)-n_y\frac{\partial n_y}{\partial x}\right)\right.$$
$$\left.+\frac{\partial V}{\partial z}\left(-n_y\frac{\partial n_y}{\partial z}-n_x\left(\frac{\partial n_x}{\partial z}-\frac{\partial n_z}{\partial x}\right)\right)\right).$$

In the main text the internal field is defined by Poisson's Eq. (7):

$$\boldsymbol{\nabla}\cdot(-\epsilon_0\underline{\underline{\epsilon}}\,\boldsymbol{\nabla}V+\mathbf{P}_{\text{flexo}})=0,\quad \underline{\underline{\epsilon}}=\epsilon_{ij}=\epsilon_\perp\delta_{ij}+\Delta\epsilon n_i n_j.$$

The two terms within the divergence operator can of course be separated to make

$$-\epsilon_0\boldsymbol{\nabla}\cdot(\underline{\underline{\epsilon}}\,\boldsymbol{\nabla}V)+\boldsymbol{\nabla}\cdot\mathbf{P}_{\text{flexo}}=0.$$

For the two-dimensional system under consideration these terms can then be written as

$$\begin{aligned}\nabla \cdot (\underline{\underline{\epsilon}} \nabla V) = {} & 2\Delta\epsilon n_x \frac{\partial n_x}{\partial x}\frac{\partial V}{\partial x} + (\epsilon_\perp + \Delta\epsilon n_x^2)\frac{\partial^2 V}{\partial x^2} + \Delta\epsilon \frac{\partial n_x}{\partial x} n_z \frac{\partial V}{\partial z} \\ & + \Delta\epsilon n_x \frac{\partial n_z}{\partial x}\frac{\partial V}{\partial z} + \Delta\epsilon \frac{\partial n_x}{\partial z} n_z \frac{\partial V}{\partial x} + \Delta\epsilon n_x \frac{\partial n_z}{\partial z}\frac{\partial V}{\partial x} \\ & + 2\Delta\epsilon n_z \frac{\partial n_z}{\partial z}\frac{\partial V}{\partial z} + (\epsilon_\perp + \Delta\epsilon n_z^2)\frac{\partial^2 V}{\partial z^2} \\ & + 2\Delta\epsilon n_x n_z \frac{\partial^2 V}{\partial x\, \partial z},\end{aligned}$$

$$\begin{aligned}\nabla \cdot \mathbf{P}_{\text{flexo}} = {} & e_1 \left\{ \left(\frac{\partial n_x}{\partial x} + \frac{\partial n_z}{\partial z} \right) \frac{\partial n_x}{\partial x} + \left(\frac{\partial^2 n_x}{\partial x^2} + \frac{\partial^2 n_z}{\partial x\, \partial z} \right) n_x \right. \\ & \left. + \left(\frac{\partial n_x}{\partial x} + \frac{\partial n_z}{\partial z} \right) \frac{\partial n_z}{\partial z} + \left(\frac{\partial^2 n_x}{\partial x\, \partial z} + \frac{\partial^2 n_z}{\partial z^2} \right) n_z \right\} \\ & + e_3 \left\{ \frac{\partial n_z}{\partial x} \left(\frac{\partial n_x}{\partial z} - \frac{\partial n_z}{\partial x} \right) + n_z \left(\frac{\partial^2 n_x}{\partial x\, \partial z} - \frac{\partial^2 n_z}{\partial x^2} \right) \right. \\ & - \left(\frac{\partial n_y}{\partial x} \right)^2 - n_y \frac{\partial^2 n_y}{\partial x^2} - \left(\frac{\partial n_y}{\partial z} \right)^2 - n_y \frac{\partial^2 n_y}{\partial z^2} \\ & \left. - \frac{\partial n_x}{\partial z} \left(\frac{\partial n_x}{\partial z} - \frac{\partial n_z}{\partial x} \right) - n_x \left(\frac{\partial^2 n_x}{\partial z^2} - \frac{\partial^2 n_z}{\partial x\, \partial z} \right) \right\}.\end{aligned}$$

[1] R. B. Meyer, Phys. Rev. Lett. **22**, 918 (1969).

[2] A. G. Petrov, in *Physical Properties of Liquid Crystals: Nematics*, edited by D. A. Dunmur, A. Fukuda, and G. R. Luckhurst (IEE, London, 2001).

[3] J. C. Jones, G. P. Bryan-Brown, E. L. Wood, A. Graham, P. Brett, and J. R. Hughes, in *Liquid Crystal Materials, Devices, and Flat Panel Displays* edited by R. Shashidhar, B. Gnade, Proceedings of SPIE (SPIE, Bellingham, WA, 2000), Vol. 3955, p.84.

[4] S. Kitson and A. Geisow, Appl. Phys. Lett. **80**, 3635 (2002).

[5] J. S. Patel and R. B. Meyer, Phys. Rev. Lett. **58**, 1538 (1987).

[6] H. P. Hinov, I. Bivas, M. D. Mitov, K. Shoumarov, and Y. Marinov, Liq. Cryst. **30**, 1293 (2003).

[7] P. Kumar and K. S. Krishnamurthy, Liq. Cryst. **34**, 257 (2007).

[8] P. Rudquist, L. Komitov, and S. T. Lagerwall, Phys. Rev. E **50**, 4735 (1994).

[9] H. J. Coles, M. J. Clarke, S. M. Morris, B. J. Broughton, and A. E. Blatch, J. Appl. Phys. **99**, 034104 (2006).

[10] A. J. Davidson and N. J. Mottram, Phys. Rev. E **65**, 051710 (2002).

[11] P. R. M. Murthy, V. A. Raghunathan, and N. V. Madhusudana, Liq. Cryst. **14**, 483 (1993).

[12] S. A. Jewell and J. R. Sambles, J. Appl. Phys. **92**, 19 (2002).

[13] A. I. Derzhanski, A. G. Petrov, Chr. P. Khinov, and B. L. Markovski, Bulg. J. Phys. **1**, 165 (1974).

[14] V. Freedericksz and V. Zolina, Trans. Faraday Soc. **29**, 919 (1933).

[15] C Gu and P Yeh, Displays **20**, 237 (1999).

[16] R. A. Ewings, C. Kischka, L. A. Parry-Jones, and S. J. Elston, Phys. Rev. E **73**, 011713 (2006).